Gold Clusters

DOI: 10.1002/ange.201102901

Generation of Small Gold Clusters with Unique Geometries through Cluster-to-Cluster Transformations: Octanuclear Clusters with Edge-sharing Gold Tetrahedron Motifs**

*Yutaro Kamei, Yukatsu Shichibu, and Katsuaki Konishi**

Molecular gold clusters with defined nuclearity and geometrical structures have attracted continuing interest, due not only to the fundamental aspects of their unique nuclearity- and structure-dependent optical and electronic properties, but also to their potential in the development of novel nanomaterials and catalysts.[1–3] Phosphine-coordinated small gold clusters (Au_n) with core nuclearities (n) ranging from 6 to 13,[4–16] which form one of the major cluster families, are typical examples. X-ray crystallographic studies have shown that these clusters generally adopt toroidal or sphere-like structures due to prominent aurophilic interactions involving the central gold atom. Examples of linear edge-shared arrays of simple polyhedra have been limited to date,[15] but recent theoretical studies have predicted that such core structures can be formed when coupled with appropriate surrounding shell (ligand) modules.[17] In this relation, current developments in cluster synthetic methods have shown the utility of multidentate ligands for selective formation of particular geometrical structures.[8–12] Herein, we report that the use of a diphosphine ligand in a cluster-to-cluster transformation through a growth/etching process leads to facile generation of two novel cluster cations $[Au_8(dppp)_4Cl_2]^{2+}$ (**2**) and $[Au_8(dppp)_4]^{2+}$ (**4**; dppp = 1,3-bis(diphenylphosphino)propane). Structural studies of these clusters revealed their unprecedented Au_8 core geometries[18] containing edge-fused gold tetrahedron motifs, which are isomeric with each other. We also highlight their geometry-dependent visible absorption and emission properties, and the selective optical response of **2** towards mercury ions.

The starting material for the growth-based strategy was $[Au_6(dppp)_4](NO_3)_2$ (**1**$(NO_3)_2$),[16] whose core contains a tetrahedral Au_4 unit plus two gold atoms bridged at opposite edges of the tetrahedron. Each of the gold atoms forming the central tetrahedron is coordinated by a single phosphine ligand, while the exo gold atoms accommodate two phosphine ligands (Figure 1). We found that growth of **1** took place readily through a reaction with the mononuclear chlorogold(I) complex $[Au(PPh_3)Cl]$, affording $[Au_8(dppp)_4Cl_2]^{2+}$ (**2**) with retention of the original tetrahedron motif (Figure 1).[19] For example, when **1**$(NO_3)_2$ was mixed with $[Au(PPh_3)Cl]$ (20 molar equiv) in methanol/chloroform at room temperature, a gradual change of the solution color from intense blue to optic pink was observed, and electrospray ionization (ESI) mass spectroscopy of the cluster species isolated from the reaction mixture showed a set of signals at approximately m/z 1648, which was unambiguously assigned to the divalent cluster cation $[Au_8(dppp)_4Cl_2]^{2+}$ (**2**) by comparison with a simulated isotopic distribution pattern (Supporting Information, Figure S1). Single-crystal X-ray diffraction analysis of the hexafluorophosphate salt **2**$(PF_6)_2$ revealed that the cluster core had a di-edge-bridged bi-tetrahedral geometry (Figure 1 and S2a),[19] which can be depicted as an extended version of the precursor cluster **1**. The two chloride ligands, each of which is bonded to one of the terminal gold atoms, are oriented in *trans* configuration with respect to the central rectangular plane composed of Au(2), Au(3), Au(6), and Au(7). The Au–Au bond lengths in the central bi-tetrahedron unit are in the range 2.65–2.87 Å, which is shorter than those involving the exo Au atoms (2.97–3.07 Å). The end-triangles involving the exo Au atoms are tilted from the central rectangular plane by 13°, and the distance of the exo Au atoms from the rectangular plane is about 0.43 Å. The ^{31}P NMR spectrum of **2**$(PF_6)_2$ in CD_2Cl_2 showed three signals at $\delta = 55.4$, 51.7, and 33.5 ppm with an intensity ratio of 1:2:1 (Supporting Information, Figure S3b), which were in agreement with the values expected from the crystal structure.

It should be noted that growth from **1** to **2** by reaction with the mononuclear complex occurred cleanly. When the reaction was monitored by UV/Vis absorption spectroscopy under dilute conditions in methanol ([**1**$(NO_3)_2]_0$/[Au-

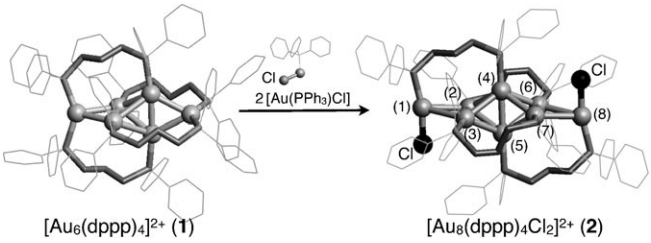

Figure 1. X-ray crystal structures of the cationic moieties of the Au_6 cluster **1** $(NO_3)_2$ and the Au_8 cluster **2** $(PF_6)_2$, and the growth from **1** to **2** through the reaction with $[Au(PPh_3)Cl]$. gold: gray spheres

[*] Y. Kamei, Dr. Y. Shichibu, Prof. K. Konishi
Faculty of Environmental Earth Science, Hokkaido University
North 10 West 5, Sapporo 060-0810 (Japan)
Fax: (+81) 11-706-4538
E-mail: konishi@ees.hokudai.ac.jp

[**] This work was partially supported by the MEXT, Grant-in-Aid for Scientific Research on Innovative Areas "Emergence in Chemistry" (20111009) and Japan Science and Technology Agency (JST), Core Research for Evolutional Science and Technology (CREST).

Supporting information for this article is available on the WWW under http://dx.doi.org/10.1002/anie.201102901.

$(PPh_3)Cl]_0 = 25.6/512\ \mu M$), the appearance of a new band at 510 nm was observed at the expense of the band at 585 nm (characteristic of **1**), with evident isosbestic points at 297, 453, and 538 nm (Figure 2). The reaction was almost complete after 4 h (Figure 2, inset), and the yield of **2**, based on the initial amount of **1** and estimated from the molar extinction coefficients (ε), was 99% after 5 h.[20] The clean reaction, with a 1:2 molar stoichiometry for **1** and $[Au(PPh_3)Cl]$ (Figure 1), suggested that the growth reaction took place smoothly, starting from one of the terminal gold atoms of **1** with subsequent ligand exchange, which allowed for facile formation of the bi-tetrahedral unit under the chelation effects of the dppp ligands. The chloride ligands may serve as end-stoppers, preventing further undesirable reactions (growth and decomposition), even in the presence of the mononuclear gold complex, to allow the selective formation of **2**. In fact, when the chloride anion of $[Au(PPh_3)Cl]$ was replaced with non-coordinating nitrate ($[Au(PPh_3)NO_3]$), no sign of the formation of Au_8 species was detected in ESI-MS and UV/Vis spectra (Supporting information, Figure S4) under similar conditions.

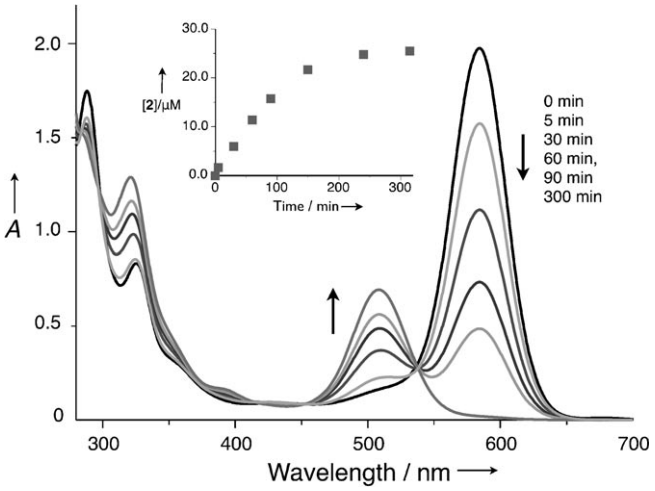

Figure 2. UV/Vis spectral changes of **1** (25.6 μM) after addition of $[Au(PPh_3)Cl]$ (20 molar equiv) in methanol at room temperature. Inset: Time course of the formation of **2** estimated from the ε values of authentic samples.

As mentioned above, the core of the Au_8 cluster cation (**2**) contained an edge-shared dimer of the gold tetrahedron unit. Interestingly, another type of Au_8 cluster was found in a ligand exchange reaction of the toroidal-shaped Au_9 cluster $[Au_9(PPh_3)_8](NO_3)_3$ (**3**)[7] with dppp. This reaction is known to result in core etching to give an Au_6 cluster ($\mathbf{1}(NO_3)_2$) as the final product,[16] but several transient Au_8 cluster species were detected during the etching process [Eq. (1)].

$$\mathbf{3}\ (Au_9) \xrightarrow{Ph_2P\frown PPh_2,\ dppp} [\ Au_8\ species\ ] \xrightarrow{dppp} \mathbf{1}\ (Au_6) \qquad (1)$$

For example, when **3** was mixed with 6 molar equivalents of dppp in dichloromethane at room temperature, the ESI-MS spectrum of the reaction mixture after 15 min showed several sets of signals due to $[Au_8(dppp)_x(PPh_3)_y]^{2+}$-type clusters ($[Au_8(dppp)(PPh_3)_5]^{2+}$, m/z 1650; $[Au_8(dppp)_2(PPh_3)_4]^{2+}$; m/z 1725; and $[Au_8(dppp)(PPh_3)_6]^{2+}$, m/z 1781) together with signals arising from $[Au_6(dppp)_4]^{2+}$ (m/z 1416; Figure 3 A(b)). After a prolonged reaction time (ca. 7 h), no signals attributable to Au_8 clusters were detected, and only signals attributable to $[Au_6(dppp)_4]^{2+}$ remained (Figure 3 A(c)). Also noteworthy is the fact that signals due to Au_9 cluster species (m/z 1290, Supporting Information, Figure S1c) were not detected throughout the ESI-MS monitoring. Therefore, it is likely that temporary binding of the dppp ligand to the Au_9 cluster in the initial stage resulted in fast etching to form Au_8. In agreement with the above observation, the UV/Vis spectrum of the reaction mixture after 15 min did not show the original Au_9 band at 442 nm, but showed bands attributable to the Au_8 clusters and **1** (Figure 3 B(b)). The band at 586 nm (**1**) developed over time, with concomitant shrinking of that at 520 nm; after 7 h, **1** was observed as the sole cluster species in the reaction mixture.

The Au_8 cluster detected as the transient species in the above etching reaction was successfully isolated by quenching the reaction through the addition of toluene, which allowed selective precipitation of the cluster species.[19] The ESI-MS spectrum of the cluster product after crystallization from dichloromethane/ether showed signals only at around m/z 1613 (Supporting Information, Figure S1d), indicating that $[Au_8(dppp)_4]^{2+}$ (**4**) was the sole cluster species isolated. X-ray crystallographic analysis of $\mathbf{4}(NO_3)_2$ revealed that the cluster core adopted edge-shared tri-tetrahedral geometry and thus had a prolate shape (Figure 4 and Figure S2b), which was clearly different from that of **2** (Figure 1).[19] The Au–Au bond lengths along the major and minor axes of the prolate spheroid were approximately 2.84 and 2.61 Å, respectively. The triad structure appeared to be retained in solution. The

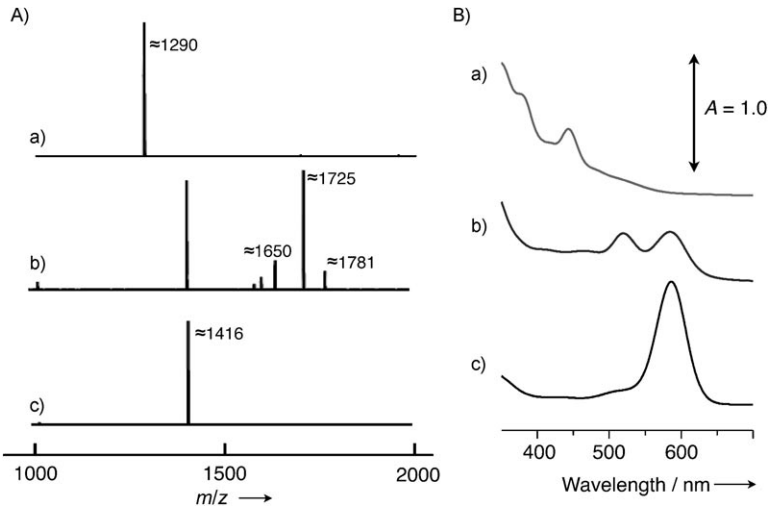

Figure 3. A) ESI-MS and B) UV/Vis monitoring of the reaction of **3** with dppp in dichloromethane. a) **3**, b) the reaction mixture after 15 min, and c) after 7 h.

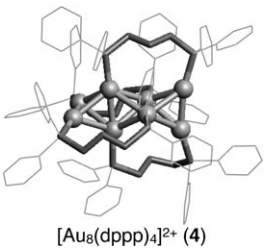

Figure 4. X-ray crystal structure of the cationic moiety of **4**$(NO_3)_2$. Gray spheres: Au.

^{31}P NMR spectrum of **4**$(NO_3)_2$ in CD_2Cl_2 showed two signals at $\delta = 62.0$ and 58.0 ppm, with the same intensities (Supporting Information, Figure S3c).

The crystal structures of **2** and **4** also demonstrated that the four dppp ligands effectively interlock the Au_8 core, contributing to stabilization of the cluster skeleton. However, the use of the dppp ligand does not seem to be the sole factor in the selective formation of Au_8 clusters. When the cluster synthesis was carried out using a conventional method ($NaBH_4$ reduction of Au^I) in the presence of dppp and nitrate or chloride ions, it resulted in the predominant formation of Au_{11}, which is ubiquitously found in the phosphine-coordinated gold cluster family.[2,4,5,9,10] Therefore, the route of growth/etching from preformed clusters may allow the emergence of unique geometric structures that are not directly accessible from metal-ion precursors.

As described above, both of the Au_8 cluster cations (**2** and **4**) exhibited absorptions in the visible region. Figure 5a shows the UV/Vis spectra of crystalline samples dissolved in dichloromethane. Although these clusters had the same nuclearity, their optical properties were obviously different. Thus, a single visible absorption band at 509 nm was observed for **2**$(PF_6)_2$, while **4**$(NO_3)_2$ exhibited a major band at 520 nm, along with a shoulder at 590 nm. Most phosphine-coordinated small gold cluster cations reported to date have icosahedron-based centered structures, including $[Au_8(PR_3)_8]^{2+}$,[4] $[Au_9(PR_3)_8]^{3+}$,[4,7] $[Au_{11}L_{10}]^{n+}$,[4,5] and $[Au_{13}L_{12}]^{3+}$,[4,8] (L = PR_3/thiolate, PR_3/halide), whose visible bands overlap with (or are sometimes obscured by) broad monotonous tailing to the near-IR region. Unlike these clusters, the Au_8 cluster cations with edge-shared gold tetrahedron motifs (**2** and **4**) exhibit discrete absorption bands in the visible region. Taking into account the absorption profiles of **1**$(NO_3)_2$ and the bi-tetrahedral $[Au_6(PPh_3)_6]^{2+}$,[15] these results imply that "isolated" visible absorption bands are likely to be a common feature of non-centered clusters containing gold tetrahedron building blocks. Theoretical work is ongoing to elucidate this point.

It should be also noted that **2**$(PF_6)_2$ showed an evident photoluminescence band at 600 nm upon excitation at 509 nm ($\phi \approx 0.1\,\%$) (Figure 5a, blue dotted line). The excitation spectrum monitored at 600 nm almost coincided with the absorption spectrum, giving a Stokes shift of approximately 0.4 eV (Figure 5a, inset). The excitation–emission relationship was similar to that reported for fluorescent small gold clusters formed in polymer matrices,[21] which suggests that the two cluster systems may be correlated with each other

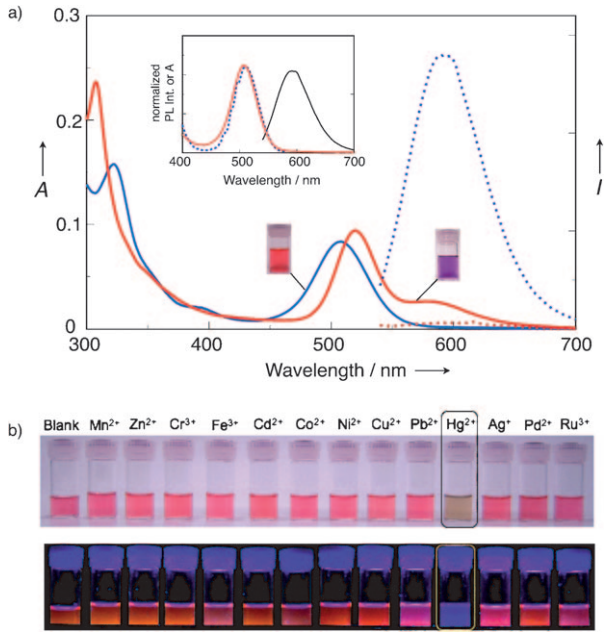

Figure 5. a) Absorption (solid lines) and photoluminescence (dotted lines) spectra of pure samples of **2**$(PF_6)_2$ (blue) and **4**$(NO_3)_2$ in dichloromethane (red) (3.1 μM) at room temperature. Inset: Normalized photoluminescence emission ($\lambda_{ex} = 509$ nm, black) and excitation ($\lambda_{ex} = 600$ nm, dotted) spectra of **2**$(PF_6)_2$, with the absorption spectrum for comparison (red). b) Chromogenic responses of **2**$(PF_6)_2$ in acetonitrile upon mixing with chloride or nitrate salts of metal ions (two molar equivalents each) under ordinary light (top) and light at 365 nm (bottom).

structurally. However, **4**$(NO_3)_2$, with a tetrahedron trimer motif, was much less photoluminescent (Figure 5a, red dotted line), again indicating that the optical properties are strictly dependent on core geometry.[22,23]

The structural difference between the two isomeric Au_8 cores was associated with their oxidation states. Thus, the formal charges of the Au_8 core units of **2** and **4** were 4+ and 2+, respectively. In this context, we found that **4** was instantly oxidized to **2** under aerobic conditions upon addition of tetraethylammonium chloride (2 molar equiv) [Eq. (2) and

$$[Au_8(dppp)_4Cl_2]^{2+}\ (\mathbf{2}) \underset{NaBH_4}{\overset{Cl^-,\ air}{\rightleftharpoons}} [Au_8(dppp)_4]^{2+}\ (\mathbf{4}) \qquad (2)$$

Supporting Information, Figure S5]. In contrast, when **2** was treated with $NaBH_4$ (1.5 molar equiv), the absorption band at 509 nm was red-shifted to around 520 nm, with the appearance of a shoulder, which is characteristic of **4** (Supporting Information, Figure S6). Thus, redox-mediated isomerization of the Au_8 core between **2** and **4** occurs smoothly in reversible fashion, demonstrating the potential of these clusters for redox-based functions.

Finally, we preliminarily tested the optical response of the Au_8 clusters to metal ions. The UV/Vis spectrum of **4**$(NO_3)_2$ upon mixing with two molar equivalents of chloride or nitrate salts of transition-metal ions (Cr^{III}, Fe^{III}, Co^{II}, Ni^{II}, Cu^{II}, Zn^{II},

Ru^{III}, Pd^{II}, Ag^{I}, Cd^{II}, Hg^{II}, and Pb^{II}) showed marked decreases in the intensity of the original absorption bands (Supporting Information, Figure S7a), suggesting that the guest metal ions induced growth or etching of the original gold cores through a metal-atom exchange reaction. Such non-specific perturbation effects of the metal ions were also observed for $\mathbf{1}(NO_3)_2$ and **3**. In contrast, $\mathbf{2}(PF_6)_2$ appeared much more inert towards the metal ions. For example, much less explicit changes in the absorption (Figure S7b) and photoluminescence spectra were observed upon the addition of most of the above metal ions. The only exception was mercury; as shown in Figure 5b, the addition of Hg^{II} to $\mathbf{2}(PF_6)_2$ in acetonitrile caused an instant color change from optic pink to brown and quenching of photoluminescence.[24] Thus, $\mathbf{2}(PF_6)_2$ serves as a chromogenic sensor that responds specifically to mercury ions.

In conclusion, we demonstrated the generation of two novel Au_8 cluster cations containing edge-shared gold tetrahedron motifs through cluster-to-cluster transformation. Spectrophotometric studies revealed that these two clusters show discrete visible absorption bands and that their optical properties depend on the core geometries associated with the oxidation states. To date, the electronic properties of metal clusters have been explained mostly in terms of the metal number (nuclearity), but the present results clearly indicate the importance of the core geometry and oxidation state. From a synthetic point of view, this study discloses the utility of post-synthetic methods utilizing growth/etching processes for the development of novel small clusters with unique geometries. The exploration of clusters of higher nuclearity with unique geometries and functions based on the rational design of ligands and reaction conditions is worthy of future investigation.

Received: April 27, 2011
Published online: June 17, 2011

Keywords: cluster compounds · geometric structures · gold · luminescence · nanomaterials

[1] *Nanoparticles-From Theory to Application* (Ed.: G. Schmid), Wiley, Weinheim, **2004**; *Modern Supramolecular Gold Chemistry* (Ed.: A. Laguna), Wiley-VCH, Weinheim, **2008**.
[2] W. Jahn, *J. Struct. Biol.* **1999**, *127*, 106.
[3] a) Y. Zhu, H. Qian, M. Zhu, R. Jin, *Adv. Mater.* **2010**, *22*, 1915; b) E. S. Andreiadis, M. R. Vitale, N. Mézailles, X. L. Goff, P. L. Floch, P. Y. Toullec, V. Michelet, *Dalton Trans.* **2010**, *39*, 10608.
[4] a) J. J. Steggerda, J. J. Bour, J. W. A. van der Velden, *Recl. Trav. Chim. Pays-Bas* **1982**, *101*, 164; b) K. P. Hall, D. M. P. Mingos, *Prog. Inorg. Chem.* **1984**, *32*, 237, and references therein.
[5] a) K. Nunokawa, S. Onaka, T. Yamaguchi, T. Ito, S. Watase, M. Nakamoto, *Bull. Chem. Soc. Jpn.* **2003**, *76*, 1601; b) K. Nunokawa, S. Onaka, M. Ito, M. Horibe, T. Yonezawa, H. Nishihara, T. Ozeki, H. Chiba, S. Watase, M. Nakamoto, *J. Organomet. Chem.* **2006**, *691*, 638.
[6] a) M. Schulz-Dobrick, M. Jansen, *Eur. J. Inorg. Chem.* **2006**, 4498; b) M. Schulz-Dobrick, M. Jansen, *Angew. Chem.* **2008**, *120*, 2288; *Angew. Chem. Int. Ed.* **2008**, *47*, 2256.
[7] F. Wen, U. Englert, B. Gutrath, U. Simon, *Eur. J. Inorg. Chem.* **2008**, 106.
[8] Y. Shichibu, K. Konishi, *Small* **2010**, *6*, 1216.
[9] M. F. Bertino, Z.-M. Sun, R. Zhang, R. L.-S. Wang, *J. Phys. Chem. B* **2006**, *110*, 21416.
[10] Y. Yanagimoto, Y. Negishi, H. Fujihara, T. Tsukuda, *J. Phys. Chem. B* **2006**, *110*, 11511.
[11] J. S. Golightly, L. Gao, A. W. Castleman Jr. , D. E. Bergeron, J. W. Hudgens, R. J. Magyar, C. A. Gonzalez, *J. Phys. Chem. C* **2007**, *111*, 14625.
[12] J. M. Pettibone, J. W. Hudgens, *J. Phys. Chem. Lett.* **2010**, *1*, 2536.
[13] V. W.-W. Yam, E. C.-C. Cheng, *Chem. Soc. Rev.* **2008**, *37*, 1806.
[14] I. O. Koshevoy, M. Haukka, S. I. Selivanov, S. P. Tunik, T. A. Pakkanen, *Chem. Commun.* **2010**, *46*, 8926.
[15] C. E. Briant, K. P. Hall, D. M. P. Mingos, A. C. Wheeler, *J. Chem. Soc. Dalton Trans.* **1986**, 687.
[16] J. W. A. van der Velden, J. J. Bour, J. J. Steggerda, P. T. Beurskens, M. Roseboom, J. H. Noordik, *Inorg. Chem.* **1982**, *21*, 4321.
[17] Y. Pei, Y. Gao, N. Shao, X. Zeng, *J. Am. Chem. Soc.* **2009**, *131*, 13619.
[18] For examples of crystallographically identified Au_8 clusters, see a) F. A. Vollenbroek, W. P. Bosman, J. J. Bour, J. H. Noordik, P. T. Beurskens, *J. Chem. Soc. Chem. Commun.* **1979**, 387; b) Y. Yang, P. R. Sharp, *J. Am. Chem. Soc.* **1994**, *116*, 6983; c) Ref. [6b].
[19] Typical synthetic procedures and crystal structure details are provided in Supporting Information. CCDC-812793 (**2**) and CCDC-812792 (**4**) contain the supplementary crystallographic data for this paper. These data can be obtained free of charge via www.ccdc.cam.ac.uk/data_request/cif (or from the Cambridge Crystallographic Data Centre, 12, Union Road, Cambridge CB21EZ, UK (fax: (+44)1223-336-033; e-mail: deposit@ccdc.cam.ac.uk).
[20] The reaction of $\mathbf{1}(NO_3)_2$ with two molar equivalents of $[Au(PPh_3)Cl]$ also occurred. However, the reaction was rather slow and the yield of **2** after 153 h, at which time the absorption attributable to $\mathbf{1}(NO_3)_2$ completely disappeared, was only around 50%. This observation suggested self-decomposition of **1** during the reaction course.
[21] a) J. Zheng, J. T. Petty, R. M. Dickson, *J. Am. Chem. Soc.* **2003**, *125*, 7780–7781; b) M. L. Tran, A. V. Zvyagin, T. Plakhotnik, *Chem. Commun.* **2006**, 2400; c) Y. Bao, C. Zhong, D. M. Vu, J. P. Temirov, R. B. Dyer, J. S. Martinez, *J. Phys. Chem. C* **2007**, *111*, 12194; d) H. Duan, S. Nie, *J. Am. Chem. Soc.* **2007**, *129*, 2412.
[22] $\mathbf{1}(NO_3)_2$ and **3** were virtually non-photoluminescent under similar measurement conditions.
[23] Geometry-dependent photoluminescence properties have been reported for isomeric $[Au_{10}Se_4]$ clusters, see: S. Lebedkin, T. Langetepe, P. Sevillano, D. Fenske, M. M. Kappes, *J. Phys. Chem. B* **2002**, *106*, 9019.
[24] Preliminary ESI-MS studies suggested the formation of mercury-containing cluster species with different nuclearity and geometry.

